

SPIN-POLARIZED SURFACE STATES ON MAX PHASE COMPOUND V₂AlC

Takahiro Ito^{1,2}, Masashi Ikemoto², Damir Pinek³, Koichiro Yaji⁴,

Shik Shin⁴, and Thierry Ouisse³

¹*Nagoya University Synchrotron radiation Research center (NUSR), Nagoya University, Nagoya 464-8603, Japan*

²*Graduate School of Engineering, Nagoya University, Nagoya 464-8603, Japan*

³*Grenoble Alpes, CNRS, Grenoble INP, LMGP, F-38000 Grenoble, France*

⁴*Institute for Solid State Physics, The University of Tokyo, 5-1-5 Kashiwanoha, Kashiwa, Chiba 277-8581, Japan*

MAX phases ($M_{n+1}AX_n$, where M is an early transition metal, A belongs to groups 13-15 and X is either C or N, $n = 1 - 3$) have recently attracted much attention due to their possible application to the production of a new class of two-dimensional (2D) systems called MXenes [1]. However, the bulk electronic structure of MAX phases has been studied mostly through *ab initio*, DFT calculations, mainly due to a lack of single crystalline samples. We have performed angle-resolved photoemission spectroscopy (ARPES) on several MAX phase single crystals to directly investigate the electronic structure of these systems [2,3]. Among the MAX phases, V₂AlC has been expected to be categorized as a high-symmetry point semi-metal with crossing point with some Dirac-like properties referred as “Dirac point (DP)” at the Fermi level (E_F) along ΓM line together with “nodal-line (NL)” around 0.2 eV from DFT calculation [3, 4]. From the recent SARPES study of V₂AlC with using a quasi - continuous - wave laser [5], the existence of the spin-polarized states has been elucidated [6]. Since the observed spin states show the anti-parallel spin splitting along the tangential axis to the larger electron pocket around the Γ point, Rashba effect [7] or the formation of the spin-polarized “drum-head surface states” have been expected to be possible origins of the spin states. To pursue the origin of the observed spin-states as well as the other spin-states if exists on V₂AlC, we have performed SARPES study with using He I light source, which is available for the spin mapping at the wide momentum space.

Figures 1(a) and (b) show the band structure near E_F and the constant energy ARPES image at 0.2 eV, comparing with the DFT band structure along the ΓM (AL) line and the DFT Fermi surface of ΓKM (AHL) plane, respectively. While the large (small) electron pocket e_L (e_s) seems to be in consistent with the previous ARPES studies [3,6], we have found an apparent dispersive feature (SS) appears between e_L and e_s bands. Since the observed SS has not been reproduced by the bulk DFT calculation, and SS dispersive feature shows similarity with the e_s band with higher binding energy shift, we expect that the origin of SS to be a “surface state”. It should be noted that the observed SS has never been observed on the previous ARPES studies with using UV synchrotron from $h\nu = 40 \sim 140$ eV [4] or laser-source of $h\nu \sim 7$ eV [6]. We expect possible origin of SS might be so called surface termination effect at the cleaved surface, which could be different from the other previous studies.

In Fig. 1(c), the SARPES spectra at the momentum cut- $m1$ to $m6$ and $p1$ to $p6$ are shown with the spin polarization along y-axis (S_y). Here, y-axis corresponds to the tangential direction to the electron pockets around the Γ point as shown in Fig. 1(b). Around the e_L pocket, S_y^- (S_y^+) polarization around 50 - 200 meV following a relatively small anti-parallel spin feature at the lower binding energy has clearly been observed around $k_x \sim \pm 0.5 \text{ \AA}^{-1}$. The

observed spin-states around the e_L pocket show a good consistency with the previous laser-SARPES study [6]. On the other hand, we have found a sizable spin polarization around SS. At the cut-m1 and m2 in Fig. 1(c), S_y^- polarization has been observed. Though the strong polarization around NL (0.2 eV at the cut-m4) might be expected to affect to the polarization in the wide momentum/energy range, appearance of S_y^- polarization below 0.1 eV at the cut-p1 and p2 should ensure the different origin of the spin-states around SS from the ones around NL (and/or e_L pocket). From the detail comparison of the relative peak position of SS between S_y^+ and S_y^- SARPES spectra, S_y^+ appears at the lower binding energy side at the cut m1(m2), while it appears at the higher side at p1(p2). Therefore it has been expected that the SS spin-polarized states might has spin-splitting which is inverted with respect to the Γ point. This result suggests that the size of spin-splitting at SS will be much smaller than one around e_L . To understand whether the mechanisms of the formation of spin-states around e_L pocket and SS are the same or not, further ARPES study choosing surface termination as well as DFT calculation of spin-texture will be performed in our future work.

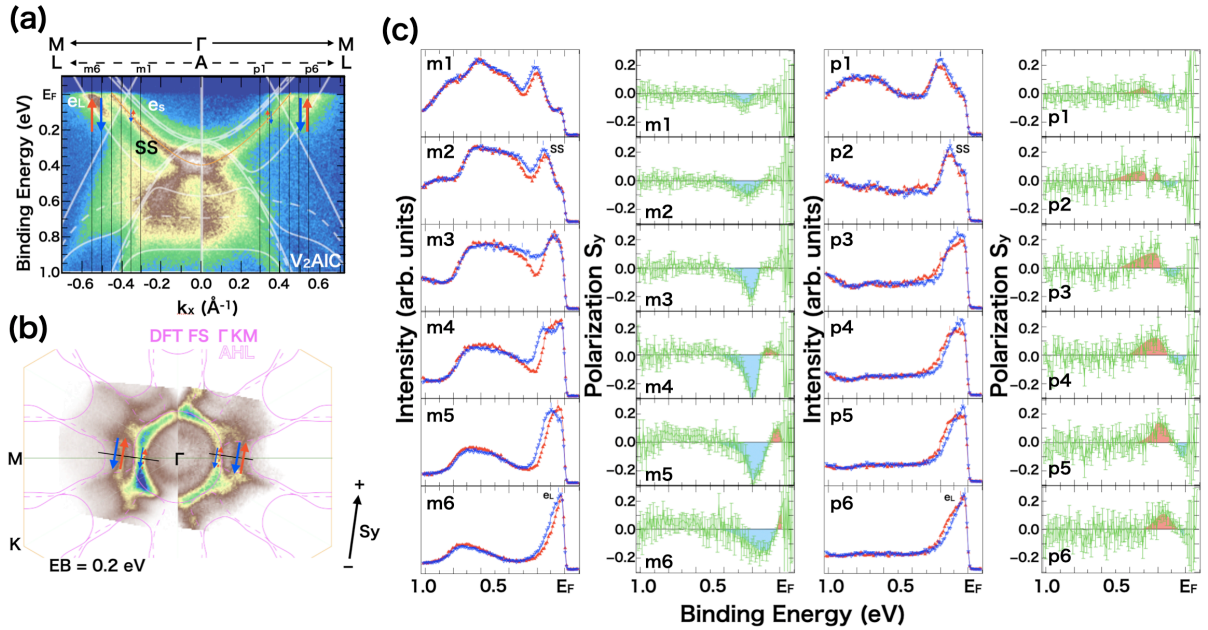


Fig. 1: (a) Band structure along ΓM line of V_2AlC . White solid (dashed) lines are obtained from DFT calculation along the ΓM (AL) line. (b) Constant energy ARPES image at 0.2 eV of V_2AlC . Purple solid (dashed) lines are Fermi surface on the ΓKM (AHL) plane obtained by the DFT calculation. The definition of spin polarization axis (S_y) is indicated by black arrow. (c) SARPES spectra (S_y^+ : \triangle ; S_y^- : \blacktriangledown) (left) and spin-polarization (right) of V_2AlC at the momentum cut from m1 (p1) to m8 (p6) in Fig. 1 (a).

REFERENCES

- [1] M. Barsoum, MAX phases (Wiley, Weinheim 2013).
- [2] T. Ito *et al.*, Phys. Rev. B **96**, 195168 (2017).
- [3] D. Pinek *et al.*, Phys. Rev. B **98**, 035120 (2018).
- [4] T. Zhang *et al.*, Nature **566**, 475 (2019).
- [5] K. Yaji *et al.*, Rev. Sci. Instrum. **87**, 053111 (2016).
- [6] T. Ito *et al.*, ACTIVITY REPORT OF SYMCHROTRON RADIATION LABORATORY 2018, 90 (2019).
- [7] V. Sunko *et al.*, Nature **549**, 492 (2017).

ABSENCE OF HYBRIDIZATION BETWEEN SPIN-POLARIZED BANDS IN QUASI-ONE-DIMENSIONAL GIANT RASHBA SYSTEM BI/INAS(110)-(2×1)

Takuto Nakamura¹, Yoshiyuki Ohtsubo^{2,1}, Ayumi Harasawa³, Koichiro Yaji³,
Shik Shin³, Fumio Komori³, Shin-ichi Kimura^{2,1}

¹*Department of Physics, graduate School of Science, Osaka University*

²*Graduate School of Frontier Bioscience, Osaka University*

³*The Institute for Solid State Physics, The University of Tokyo*

Surface electronic structure with helical-spin texture thanks to spin-orbit interaction (SOI) have been extensively studied not only for basic physics but also for applications to spintronic devices [1-3]. In order to describe such system, a simple spin texture, one band has only one spin polarization orientation and orbital character, has been widely used in the earlier studies. However, recent spin and angle-resolved photoelectron spectroscopy (SARPES) and first principles calculation studies have been revealed that the spin texture of these systems are actually not so simple, but strongly entangled with the orbital components of the surface band structure [4-6]. Spin inversion and gap opening due to hybridization between spin-polarized bands has also been reported about 2D Rashba system such as Bi/Ag quantum well [6, 7]. Although such studies have been carried out extensively for 2D systems, its extension to one-dimensional (1D) or quasi-1D (Q1D) systems were not achieved yet. In this project, we observed spin-orbital texture on a giant Rashba-type spin-splitting Q1D system Bi/InAs(110)-(2×1) [8] by using laser-based SARPES equipment [9].

Figure 1 (a) shows spin-integrated ARPES band mapping of the Bi/InAs(110)-(2×1) surface along Q1D chain direction with *p*- polarized photons. Two parabolic bands, S1 and S2, with a top away from the center of the surface Brillouin zone ($k = 0 \text{ \AA}^{-1}$) were observed near the Fermi level. ARPES constant energy contour (not shown) indicated the anisotropic, Q1D character of both S1 and S2. From the in-plane spin-resolved measurement as shown in figure 1 (b), both parabolic bands show clear spin polarization, and the signs of the spin polarizations are the opposite to each other. These results are consistent with our previous data [7], suggests the spin splitting due to Rashba-type SOI.

In order to clarify the hybridization effect of the two spin-polarized bands, we extracted the energy distribution curves (EDCs) from figure 1 (a) and show the results in figure 1 (d). The peak positions of the S1 (S2) band are indicated by a filled (open) triangles. Although the two bands are crossing each other at $k = 0.21 \text{ \AA}^{-1}$, no energy gap was observed. Moreover, spin-resolved EDCs as shown in figure 1 (e) indicated no spin-inversion nor interference at the crossing point ($k = 0.21 \text{ \AA}^{-1}$). These results suggest that there is no band modulation in Bi/InAs(110)-(2×1) surface, such as spin flipping or spin gaps opening, due to the hybridization between the spin-polarized bands. This behaviour is different from that of the known 2D Rashba systems such as Bi/Ag quantum wells [6,7].

We are currently tracking the detailed changes in orbital components and spin polarization at the initial state in combination with the density-functional-theory calculation, in order to understand this lack of hybridization between Rashba-type spin-polarized surface bands.

REFERENCES

- [1] É. I. Rashba, Sov. Phys.-Solid State **2**, 1109 (1960).
 [2] M. Z. Hasan and C. L. Kane, Rev. Mod. Phys. **82**, 3045 (2010).
 [3] A. Manchon *et al.*, Nature Mat. **14**, 871 (2015).
 [4] K. Yaji *et al.*, Nat. Commun. **8**, 14588 (2017).
 [5] K. Kuroda *et al.*, Phys. Rev. B **94**, 165162 (2016).
 [6] R. Noguchi *et al.*, Phys. Rev. B **95**, 041111(R) (2017).
 [7] H. Bentmann *et al.*, Phys. Rev. Lett. **108**, 196801 (2012).
 [8] T. Nakamura *et al.*, Phys. Rev. B **98**, 075431 (2018).
 [9] K. Yaji *et al.*, Rev. Sci. Instrum. **87**, 053111 (2016).

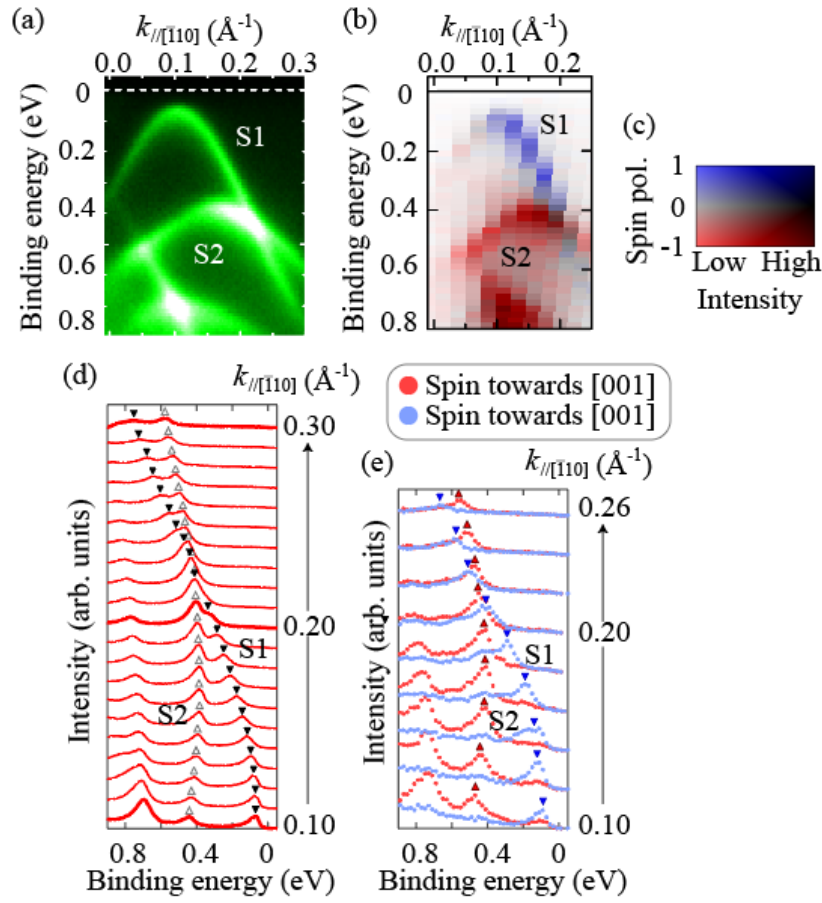


Figure 1. Surface electronic structure of Bi/InAs(110)-(2x1) surface. (a) Spin-integrated and (b) spin-resolved ARPES band mapping along Bi chain direction. Spin-direction was set to in-plane chain normal ($k_{//[001]}$) direction. (c) The 2D color code for (b). blue-red color corresponds to spin polarization and the contrast of the color to the intensity of photoelectrons. (d) Spin-integrated and (e) spin-resolved EDCs. All data were measured at 45K.

TOPOLOGICAL SURFACE STATE MODIFIED BY ADSORPTION OF ORGANIC DONOR MOLECULE

Tatsuya Kitazawa¹, Koichiro Yaji², Kosuke Shimozawa¹, Hiroshi Kondo¹, Takayoshi Yamanaka¹, Hiroshi Yaguchi¹, Yukiaki Ishida², Kenta Kuroda², Ayumi Harasawa², Takashi Iwahashi³, Yukio Ouchi³, Fumio Komori², Shik Shin², and Kaname Kanai¹

¹*Department of Physics, Faculty of Science and Technology, Tokyo University of Science*

²*Institute for Solid State Physics, The University of Tokyo*

³*Department of Materials Science and Engineering, Tokyo Institute of Technology*

Topological insulators (TIs) have attracted much attention in quantum matter physics. Topological surface states (TSS) have a helical-spin texture, in which the spin-locked electrons are topologically protected against the backscattering from nonmagnetic impurities due to time reversal symmetry¹. This property of TSS will be important in next-generation spintronic devices because it will allow lower-energy electronic transport. Thus, controlling the TSS by creating topological interfaces with other materials is vital for using TIs in spintronic devices. In 2016, Tu *et al.* reported a topological p-n junction on the surface of $\text{Bi}_{2-x}\text{Sb}_x\text{Te}_{3-y}\text{Se}_y$, a three-dimensional TI fabricated by using electron-accepting organic molecule F_4 -tetracyanoquinodimethane (TCNQ), and they achieved on-off switching of charge current flow originating from TSS², suggesting that electronic functional organic molecules are suitable for TI spintronic devices. Recently, there have been several studies of the TI interface with organic molecules toward using TIs in spintronic devices. Caputo *et al.* examined the cobalt phthalocyanine (CoPc)/ Bi_2Se_3 interface³ and observed a slight shift in the Dirac point (DP) to higher binding energy by angle-resolved photoemission spectroscopy (ARPES) experiments, indicating charge transfer from CoPc to Bi_2Se_3 . This means that the CoPc/ Bi_2Se_3 interface is a chemisorption system. However, a negligible shift in the Bi 4f core levels was observed by X-ray photoemission spectroscopy (XPS), indicating little charge transfer at the interface. These experimental results contradict each other. The interface between TCNQ, a typical electron acceptor, and Bi_2Se_3 was studied by Pia *et al.*⁴ They observed a DP shift to higher binding energy by ARPES and a shift of the Bi 4f core level toward lower binding energy accompanied by TCNQ deposition by XPS measurements. These results indicate that there is a chemical interaction between adsorbed TCNQ and Bi_2Se_3 . Therefore, studies of the interfacial electronic structure of the TCNQ/ Bi_2Se_3 interface should consider chemical interactions, such as charge transfer.

These earlier experimental studies of the interface between the organic molecules and the TI surface have led to contradictory interpretations of the interactions at the organic molecule/TI interfaces. Little attention has been paid to the electronic structure of molecular layers, although this is essential for properly evaluating the interfacial electronic structure. Also, it can be pointed out that there are few reports on the electron donating molecules (n-type dopant) although some researches on the electron-accepting molecules (p-type dopant) like TCNQ and its derivatives have been reported.

In the present work, we directly observed the electronic structure both of the molecular layers and the TI surface to fully understand the influences on the TSS upon the adsorption of the molecules. We focused on the interface between tetrathianaphthacene (TTN) and Bi_2Se_3 .

Bi_2Se_3 has been extensively investigated as a prototypical TI. A Bi_2Se_3 single crystal comprises five-atom layers (Se-Bi-Se-Bi-Se) stacked along the [111] direction, which are known as quintuple layers (QLs). The QLs are attached to each other by weak van der Waals (vdW) forces and the interlayer gap between QLs is called the vdW gap. We chose Bi_2Se_3 because it has a single Dirac cone at the Γ point in the (111) surface Brillouin zone and a wide band gap of ~ 0.3 eV. This simple electronic structure allows us to trace the DP shift accompanied by the molecular deposition easily. To create the organic molecular layer/TI interface, we vacuum deposited TTN onto Bi_2Se_3 . TTN is a π -conjugated molecule containing

four electron rich sulfur atoms and has a strong donor nature by a small ionization energy of ~ 4.4 eV. TTN functions as a strong n-type dopant for Bi_2Se_3 because the Fermi level of Bi_2Se_3 is lower than the highest occupied molecular orbital of TTN. The role of donor organic molecules on the TI surface has not been investigated thoroughly, in contrast to acceptor organic molecules or n-type dopants, like alkali metals and other inorganic materials. Organic molecules have the advantages of requiring lower-cost methods for creating the interface with TI and having a lower risk of intercalation into the bulk. Thus, organic molecules are good candidates for manipulating the TSS.

In this work, we observed the entire electronic structure of the TTN/ Bi_2Se_3 interface by examining the TTN thickness dependence of the interfacial electronic state using UPS, XPS, and ARPES.

Figure 1 shows the Fermi surfaces and the energy band dispersions measured at the TTN/ Bi_2Se_3 interface for various TTN thicknesses by ARPES. For the 5Å-thick TTN, the Dirac point (DP) shifted toward higher binding energy ($E-E_F = -0.42 \pm 0.02$ eV) and the Fermi surface area of TSS increased. The hexagonal warping of the Fermi surface was also observed. We also observed the emergence of a new state just below the Fermi level with a parabolic band dispersion and hexagonal Fermi surface upon TTN deposition. This new state was identified as the two-dimensional electron gas state (2DEG) originating from the bulk conduction band, which is induced by the band-bending derived from the increase in the number of TSS electrons.

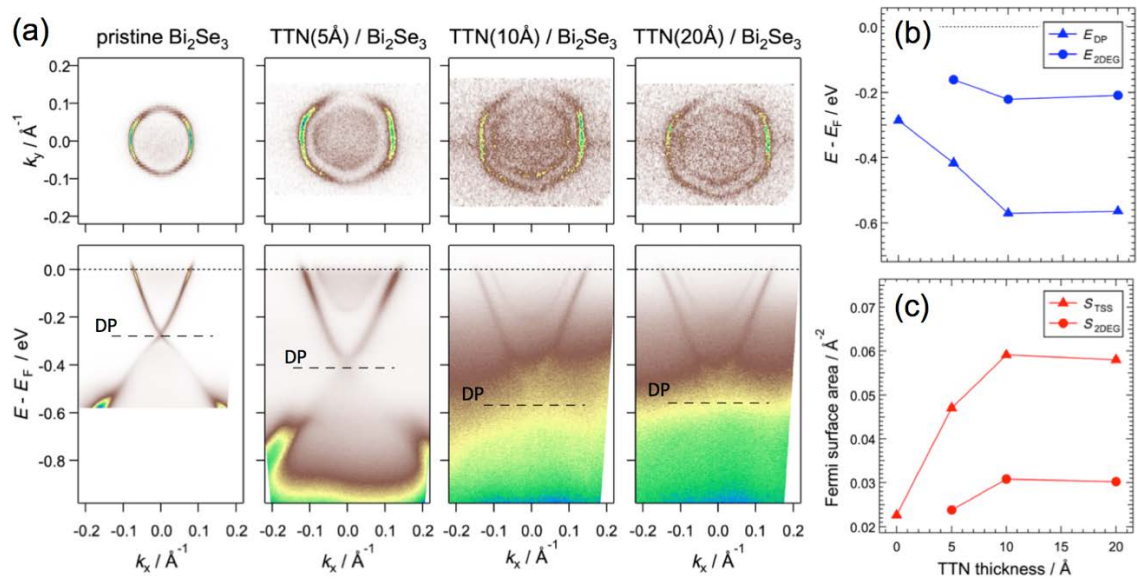


Fig. 1: Development of the electronic structure at the TTN/ Bi_2Se_3 interface. a) ARPES spectra of Bi_2Se_3 and a TTN molecular layer of various thicknesses, showing the Fermi surface and the energy band dispersion of photoemission intensity. The dashed lines labeled DP represent the energy of DPs. These ARPES spectra are acquired along the momentum line slightly off the Γ K line in the surface Brillouin zone. b) Positions of the DP (E_{DP}) and the bottom of 2DEG band dispersion (E_{2DEG}) and c) the Fermi surface area of TSS (S_{TSS}) and 2DEG (S_{2DEG}).

REFERENCES

- [1] P. Roushan *et al.*, Nature **460**, 1106 (2009).
- [2] N. H. Tu *et al.*, Nat. Comm. **7**, 13763 (2016).
- [4] M. Caputo *et al.*, Nano Lett. **16**, 3409 (2016).
- [5] A. D. Pia *et al.*, Chem. Phys. Chem. **19**, 2405 (2018).

INVESTIGATION OF TOPOLOGICAL PROPERTIES IN SUPERCONDUCTING TASE₃

Chun Lin¹, Ryo Noguchi¹, Kenta Kuroda¹, Koichiro Yaji¹, Ayumi Harasawa¹, Shik Shin¹,
 Atsushi Nomura², Masahito Sakoda³, Masakatsu Tsubota⁴, Satoshi Tanda³,
 and Takeshi Kondo¹

¹*The Institute for Solid State Physics, The University of Tokyo*

²*Department of Physics, Tokyo University of Science*

³*Department of Applied Physics, Hokkaido University*

⁴*Department of Physics, Gakushuin University*

In recent years, a great deal of research activities are associated with the quantum materials characterized by either the low dimensionality [1] or the electronic topology [2]. TaSe₃ is known as a quasi-1D semimetal with layered chain-like structure [Fig. 1 (a)] and has been extensively discussed in the early ages for its superconducting properties and the absence of charge density wave (CDW) [3]. These characteristics make it distinct from other transition-metal trichalcogenides, which typically undergo multiple CDW transitions [3]. As shown in Fig. 1 (b), it is considered that the absence of CDW stems from the relatively poor nesting conditions in TaSe₃ due to its more 3D-like electronic structure and CDW may be induced by Cu intercalation [4,5] or in mesowires [6], both of which are expected to reduce the dimensionality. A recent first-principle calculation indicate that TaSe₃ actually belongs to a strong topological insulator (TI) phase and moreover predict intriguing topological phase transitions among strong TI, weak TI, Dirac semimetal, and normal insulator phases through a slight change of lattice parameters, as demonstrated in the topological phase diagram of Fig. 1 (c) [7]. Therefore, TaSe₃ offers a simple system to study the interplay between superconductivity and topological phases, and the possibility of selecting different topological phase by changing physical parameters (temperature, element substitution etc.).

A direct investigation of the electronic structure of TaSe₃ via angle-resolved photoemission spectroscopy (ARPES) is consequently indispensable to elucidate its novel topological properties. We have conducted laser-based spin-resolved ARPES (SARPES) measurements at the Institute for Solid State Physics, the University of Tokyo last year and reported the first unambiguously observation of the electronic structure of TaSe₃ and the possible topological surface states (TSSs) [8]. In present study, we show the high-resolution band structure of the possible TSSs and confirm that these surface states are indeed spin-momentum locked. Therefore, our results reveal a well-established TI phase in quasi-1D TaSe₃.

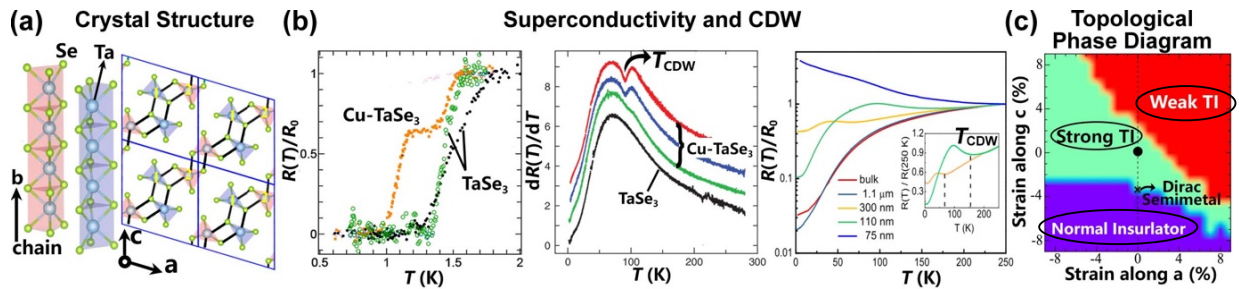


Fig. 1 (a) Crystal structure and unit cell of TaSe₃ [7]. (b) Superconductivity in pure and Cu-doped TaSe₃ (left) [4], CDW signature in Cu-doped TaSe₃ (middle) [5], and direct observation of CDW in mesowire TaSe₃ with

hundreds of nano-meters in width (right) [6]. (c) Topological phase diagram of TaSe₃ including strong topological insulator (TI), weak TI, Dirac semimetal, and normal insulator phases [7].

Figures 2 (a,b) show the 3D Brillouin zone [7] and our recently calculated TSSs at the X point on (-101) surface. Figure 2 (c) is the schematic of the experimental ARPES setup and the typical sample size. In Figs. 2 (d,e), we present the high-resolution Fermi surface and the band dispersion at the X point. The observed sharp and high-intense features near E_F are nicely consistent with our calculations in Fig. 2 (b). To further confirm whether the sharp electronic states are spin-polarized, Fig. 2 (f) shows one typical spin-revolved energy distribution curves and the corresponding spin polarization at a momentum position indicated by the dash line in Fig. 2 (e). Taking advantage of our high-resolution SARPES, the spin splitting is clearly observed for the spin up and spin down states, uncovering a spin polarization of $\sim 20\%$. We confirmed a reversal of the spin polarization for an opposite momentum position. Therefore, our results elucidate the spin-momentum locked TSSs in TaSe₃.

To sum up, we performed high-resolution SARPES measurements on TaSe₃ focusing on the surface states, the results confirm the spin-momentum locked TSSs and hence a TI state.

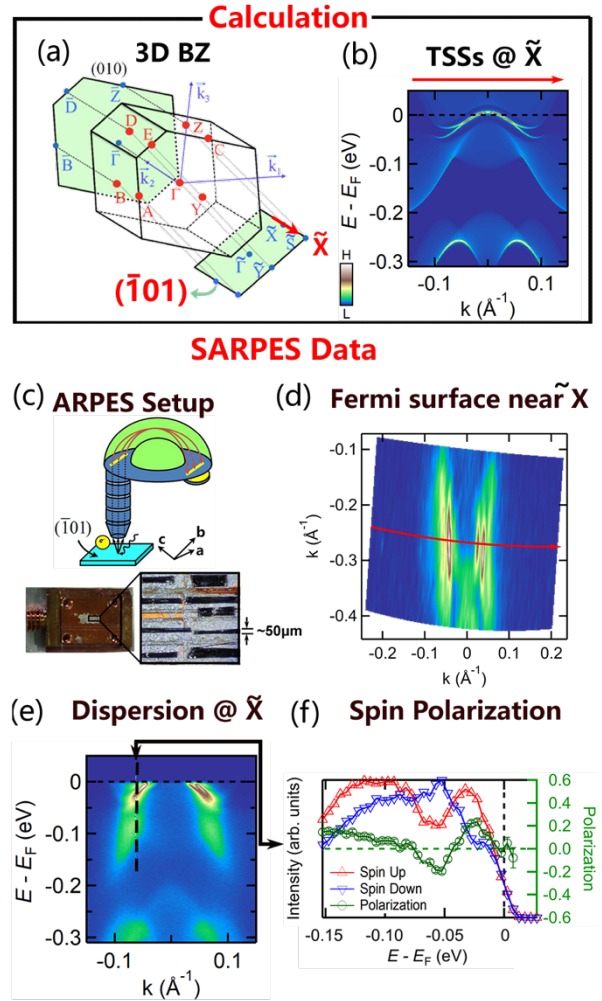


Fig. 2 (a) 3D Brillouin zone (BZ) of TaSe₃ [7]. (b) Calculated topological surface states (TSSs) at the X points on (-101) surface [7]. (c) ARPES setup. Typical samples size is $\sim 1 \times 0.05 \times 0.01$ mm³. (d) Observed surface-state Fermi surface on (-101) surface near the X point at 10 K. (e) The corresponding high-resolution dispersion at the X point with momentum position indicated by the red arrow in (d). (f) Spin polarization at the momentum position indicated by a dash line in (e). Red and blue curves are energy distribution curves of spin up and spin down states, respectively.

REFERENCES

- [1] Y. Liu, et al., Nat. Rev. Mater. 1, 1 (2016).
- [2] X.-L. Qi, S.-C. Zhang, Rev. Mod. Phys. **83**, 1057–1110 (2011).
- [3] P. Monceau, Adv. Phys. **61**, 325 (2012).
- [4] A. Nomura, et al., EPL. **124**, 67001 (2019).
- [5] A. Nomura et al., EPL. **119**, 17005 (2017).
- [6] J. Yang et al., ArXiv190609527 (2019).
- [7] S. Nie et al., Phys. Rev. B **98**, 125143 (2018).
- [8] C. Lin et al., ISSP Activity Report of Synchrotron Radiation Laboratory (2018).

ANGLE- AND SPIN-RESOLVED PHOTOEMISSION SPECTROSCOPY RESEARCH ON TYPE-II WEYL SEMIMETAL WTe₂

Yuxuan Wan^{1,2}, Lihai Wang³, Keisuke Koshiishi¹, Masahiro Suzuki¹, Peng Zhang²,
Jaewook Kim⁴, Kenta Kuroda², Koichiro Yaji², Ryo Noguchi², Ayumi Harasawa², Shik Shin²,
Atsushi Fujimori¹, Sang-Wook Cheong³, Takeshi Kondo²

¹*Department of Physics, The School of Science, The University of Tokyo*

²*The Institute for Solid State Physics, The University of Tokyo*

³*The Center for Quantum Materials Synthesis, Rutgers University*

Introduction

So far, no example of Weyl fermions has been observed in particle physics research. On the other hand, some topological materials are expected to host electrons behaving as Weyl fermions. These materials, called Weyl semimetals, have spin-polarized bands with cone-like linear dispersions with zero-mass near Weyl points, which are generated when either time-reversal or space-inversion symmetry is broken. The Weyl points are topologically protected, and intriguingly, topological surface states connect a pair of Weyl points with opposite chirality, forming arc-like Fermi surface (Fermi arc).

In some Weyl semimetals, the hole- and electron-like pockets touch each other at several Weyl points. These kinds of Weyl semimetals are called type-II Weyl semimetals, and WTe₂ we study here is one of such candidates. In WTe₂, the space inversion symmetry along *c*-axis is broken, thus the top and bottom surfaces should be different [1-3]. Theoretical calculations predict distinct Fermi arc states for these two surfaces [4], which require detailed experimental investigation.

Experiment

The single crystals of WTe₂ with large domains were grown via the iodine vapor transport method [4]. Comparing with previous studies, the single crystals have a much larger domain size. We developed a new method to obtain a pair of samples with opposite polar surfaces as shown in Fig. 1, namely “sandwich method”. A single crystal of sample was fixed on a metal substrate with silver paste as usual ARPES experiment. Then we applied silver paste on the top surface of the sample and covered it with another metal substrate. After heating the sample until the silver paste was hardened, we separated the two substrates to cleave the sample. The two pieces of sample would expose different surfaces.

The experiment was carried out with the spin-resolved laser ARPES (SARPES) at ISSP, the University of Tokyo. The light source is 7 eV laser from KBBF crystal. We measured two kinds of

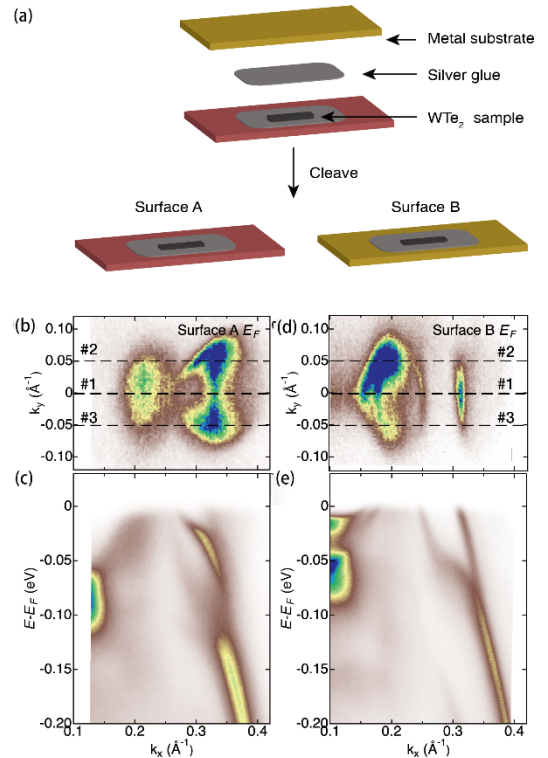


Fig.1 (a) The method to get a pair of samples with polar surfaces. (b) and (c) The Fermi surfaces on both the polar surfaces by laser ARPES. (d) and (e) Band dispersions along high symmetry cuts.

surfaces of WTe_2 : surface A and B. We used the 7 eV laser ARPES to map the energy contours and measured the band structures. We found two kinds of ARPES results on the polar surfaces. SARPES measurements on candidate topological surface states were taken after the ARPES measurements. We distinguished surface states from bulk states.

Results

We measured two kinds of surfaces of WTe_2 : surfaces A and B with 7 eV laser-ARPES. In Fig. 1 (b)-(e), we can see the arc-like surface states on both surface A and B. The surface states of the opposite surfaces are different because of the lack of inversion symmetry as expected.

Figure 2 shows the SARPES results of the candidate topological surface states. The spin polarization of bulk bands inverted on the polar surfaces, while surface states keep the same direction. We also found a surface resonance state generated by the mixture of the surface state and the hole pocket, suggesting that the hole and electron pocket also connect below the Fermi level, which is not predicted by theoretical studies. The band structures are linear near the contact point with a Dirac-like cone.

We observed two kinds of surfaces of type-II Weyl semimetal WTe_2 with laser-ARPES. Clear surface states which connect the bulk hole- and electron-like pockets could be seen. By SARPES measurements, we found that the surface states are all spin-polarized, which are compatible with topological Fermi arcs.

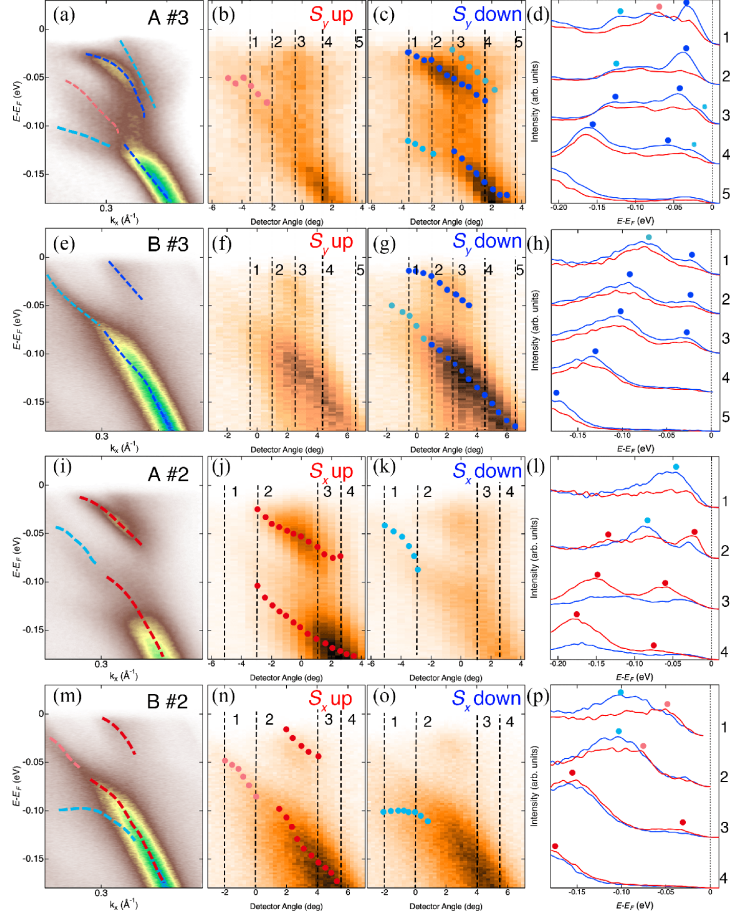


Fig.2 (a) and (e) The ARPES images of cut 3 on surface A and B, respectively. The red (pink)/blue (light-blue) dashed lines indicate the band dispersions with s_y -up/down polarization. (b),(c),(f) and (g) Laser-SARPES images for s_y -up and down.(d) and (h) Energy distribution curves (EDCs) for up (red) and down(blue) along dashed line in (b), (c), (f), and (g). The marks indicated the positions of the peaks: light-blue and pink rounds for bulk states and blue and red for surfaces, which are also plotted on (b), (c), (f), and (g). (i)-(p) Similar set for spin x component along cut 2 on surface A and B.

REFERENCES

- [1] A.Soluyanov *et al.* *Nature* 527.7579 (2015).
- [2] Y.Wu *et al.*, *Phy. Rev. B* 94, 121113(R) (2016).
- [3] F.Y.Bruno *et al.*, *Phy. Rev. B* 94, 121112(R) (2016)
- [4] W.Zhang *et al.*, *Phy. Rev. B* 96, 165125 (2017)

DEVELOPMENT OF TIME-, SPIN- AND ANGLE-RESOLVED PHOTOEMISSION SPECTROSCOPY MACHINE AT ISSP

K. Kawaguchi, K. Kuroda, Z. Zhao, A. Harasawa, K. Yaji, R. Noguchi, S. Tani,
M. Fujisawa, S. Shin, F. Komori, Y. Kobayashi, T. Kondo
The Institute for Solid State Physics (ISSP), The University of Tokyo

Spin- and angle-resolved photoemission spectroscopy (SARPES) is a powerful technique to directly access spin-polarized electronic structures [1]. In 2014, We have newly built the laser-SARPES machine at ISSP, which is based on the 6.994-eV laser generated by KBBF non-linear crystal and the double VLEED-type spin detector [2]. Thanks to the high-flux light source as well as the high-efficiency of the detectors, our SARPES machine enables us to reveal the various spin-polarized states and the related phenomena.

Recently, we have started to a project to upgrade our laser-SAPRES machine by combining femtosecond laser pulses to perform pump-probe time-resolved SARPES (tr-SARPES). In contrast to the standard SARPES, this technique allows us to investigate the non-equilibrium spin-polarized electronic states and its spin dynamics disentangled from the charge dynamics. We have installed a new 10.7 eV-laser pulse developed by Kobayashi group of ISSP [3], which is based on the Yb-doped fiber with the high repetition rate (1 MHz). The 10.7 eV laser is generated by the third harmonic generation of the 347-nm driver in Xe gas. The high-energy probe pulse will cover the entire first Brillouin Zone (BZ), which is a great advantage compared to the conventional 6 eV-lasers based on Ti:sapphire laser.

In this activity report, we report the status of the machine development. At this stage, we have detected the SARPES signals probed by 10.7 eV laser. We here will show its demonstrations on polycrystalline-Au, and Bi/Si (111) films.

We characterize energy resolution by measuring polycrystalline gold plate (Fig. 1). By fitting analysis of the energy distribution curves (EDCs) by a Fermi-Dirac function convoluted by Gaussian, we estimate the energy broadening of the laser itself to be 20 meV. This value is reasonable if we consider the band width of the fundamental laser generated by the Yb-doped fiber. We also find that there is no significant space charging effect, which is the best advantage of the high-repetition laser.

Next, we mapped the band dispersions of Bi/Si (111) film. Fig. 2(a) shows the observed Fermi-surfaces covering the

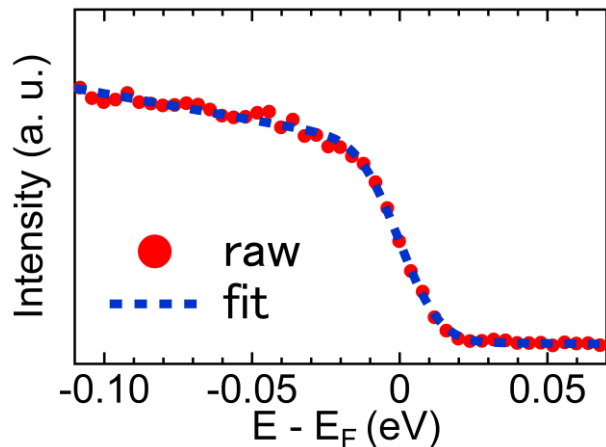


Fig. 1: EDCs recorded by 10.7 eV laser on the polycrystalline gold plate at 17 K. Dashed curve is a fitting function to deduce the energy resolution of the laser pulse itself.

BZ. We also measured the clear band dispersions of Bi/Si (111) in wide energy-momentum windows [Fig. 2(b)]. This guarantees that our laser system is stable for SARPES and ability to investigate the spin-polarized band structure for entire first BZ. We are now installing the pump pulses to perform the pump-probe tr-SARPES measurement.

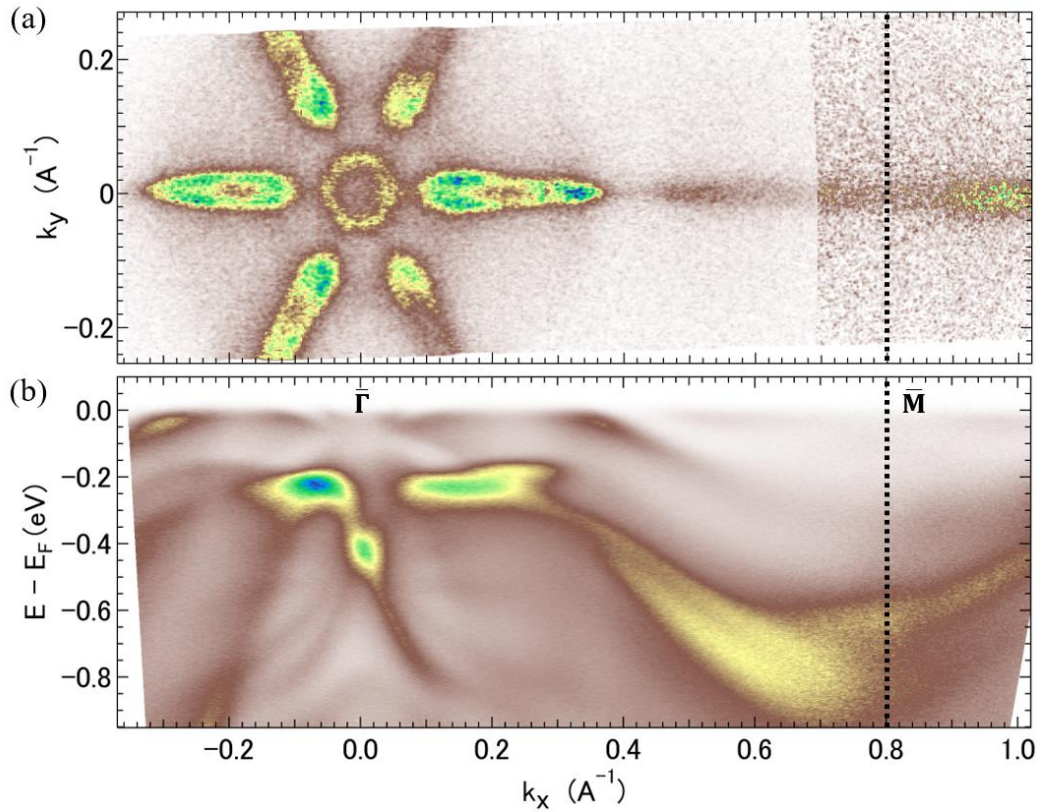


Fig. 2: (a) The Fermi surface of Bi/Si (111) films. 10.7 eV laser is p-polarization set up, and analyzer slit is along Γ M line. (b) Band dispersion image along Γ -M direction.

References:

- [1] J. H. Dil, *Electron. Struct.* **1**, 023001 (2019).
- [2] K. Yaji *et al.*, *Rev. Sci. Instrum.*, **87**, 053111 (2016).
- [3] Z. Zhao *et al.*, *Opt. Exp.* **25**, 13517 (2017).

THE WEAK TOPOLOGICAL INSULATOR STATE IN ZRTE₅

Peng Zhang¹, Ryo Noguchi¹, Kenta Kuroda¹, Chun Lin¹, Kaishu Kawaguchi¹, Koichiro Yaji², Ayumi Harasawa¹, Simin Nie³, Hongming Weng⁴, V. Kandyba⁵, A. Giampietri⁵, A. Barinov⁵, Qiang Li⁶, G.D. Gu⁶, Shik Shin^{7,1}, and Takeshi Kondo¹

¹*Institute for Solid State Physics, University of Tokyo, Kashiwa, Chiba 277-8581, Japan.* ²*Research Center for Advanced Measurement and Characterization, National Institute for Materials Science, Tsukuba, Ibaraki 305-0003, Japan.* ³*Department of Materials Science and Engineering, Stanford University, Stanford, California 94305, USA.* ⁴*Beijing National Laboratory for Condensed Matter Physics and Institute of Physics, Chinese Academy of Sciences, Beijing 100190, China.* ⁵*Elettra - Sincrotrone Trieste, Basovizza, Italy.* ⁶*Condensed Matter Physics and Materials Science Department, Brookhaven National Laboratory, Upton, NY, USA.* ⁷*Office of University Professor, University of Tokyo, Kashiwa, Chiba 277-8581, Japan*

Two distinct topological insulators exist in three dimensions: strong topological insulator (STI) and weak topological insulator (WTI). Among them, STI have been widely studied in the past decades both in theories and experiments. There are 2D spin-momentum locked Dirac cones on all the surfaces, in which the perfect backscattering is prohibited, while general scattering away from 180 degree still exists. On other hand, there are many theory studies on WTI but experiments are still rare. WTI host surface states only on the side surfaces. They are thought to be weak since two adjacent layers in even-layer WTI may couple with each other, leading to a topologically trivial phase. However, it is found that WTI surface states are actually robust as a results of delocalization. Furthermore, surface bands of WTI generally have a quasi-1D dispersion. Similar to the quantum spin Hall edge states, there are less scattering channels than STI, and smaller scattering at the side surface is expected. However, experiments on surface states of WTI are rare, due to the difficulty to prepare a large and uniform side surface of layered materials. Cleavage is generally useful for top surface, and such techniques proved its power on STI. In nature, most materials can only be cleaved from top surface, and it is difficult to prepare a side surface. The only example is Bi₄I₄, which has two cleaved surface at the same time (specially) [1]. ZrTe₅ is another candidate of WTI [2]. Although there are some spectroscopic studies on the top surface, there is no study on the side surface. The key evidence for WTI of ZrTe₅, the results from side surface, is missing, and the properties of the surface band is absent.

ZrTe₅ has a quasi-1D crystal structure. The layer distance for the top surface is ~ 7.3 Å, and it is ~ 6.9 Å for the side surface. As a result of the large layer distances, in principle, it should be possible to cleave both surfaces. However, Te-Te bonding exists between adjacent layers for the side surface, making it much more difficulty to cleave than the top surface stacked by van der Waals forces. We successfully cleaved the side surface of WTe₅, and measured its band structure with laser ARPES. We resolved a Fermi surface only dispersing along the chain direction (a), as displayed in Fig. 1a. The ARPES intensity plot along k_a shows a hole-like band. By comparing with the calculations [2], we found this band should be the surface band. The spin polarization is expected for the surface band.

We measured two pairs of EDCs (Fig. 1a) by spin-resolved ARPES from three different samples. The k_a locations are also shown in Fig. 1b. The spin polarization curves along the b , a and c directions are displayed in Fig. 1c - e. In each panel of Fig. 1c - e, the five curves with the same color (blue or red) are taken at two different k_b ($k_b \sim 0$ and 10 , indicated in Fig. 1a)

from three samples (one sample at only $k_b \sim 0$, in total $6 - 1 = 5$ curves). These five curves show no obvious difference, confirming the repeatability of the measurements. We notice that the spin polarization curves in the background range (< -0.15 eV) are not zero but have offsets. Such constant polarization in the background may come from the asymmetry of the spin + and spin - channels, or may come from the matrix-element effect in the photoemission process, which is often observed in spin-resolved ARPES. We averaged the five polarization curves with the same color in Fig.1c - e, and subtracted the resulting curves by a constant to remove the background polarization. The results are displayed in Fig.1f - h. It is clear that the spin is polarized along b direction, tangent with the Fermi surface, forming the quasi-1D spin-momentum locking pattern. Our results prove the existence of topological surface states on the side surface, and the weak topological insulator nature of ZrTe₅.

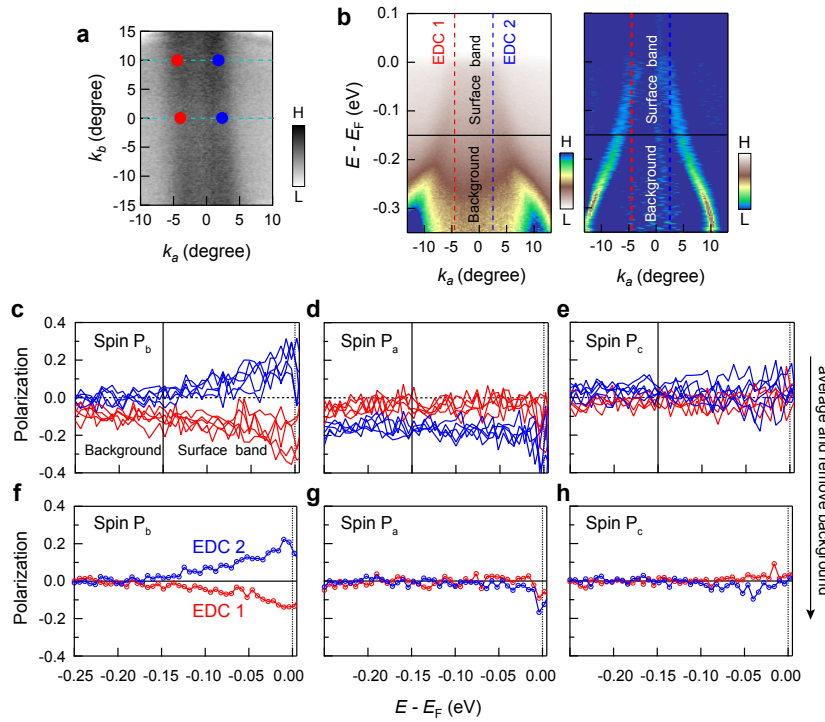


Figure 1. Spin polarization calibration. (a) Fermi surface of the side surface. The red and blue dots indicate the locations in k -space of the spin-polarized EDCs in (c - h). (b) Intensity plot of the band structure along k_a and its MDC curvature plot. The red and blue lines indicate the k_a locations of the spin-polarized EDCs. Due to the quasi-1D feature of the Fermi surface, the band structure at $k_b \sim 0$ and $k_b \sim 10$ in (a) are basically the same. (c - e) Raw spin polarization curves along b , a and c directions measured at the indicated locations in (a) and from different samples. The polarization curves at the same k_a are almost the same (independent of k_b locations or samples). So the curves are just distinguished by their k_a values with red and blue colors. (f - h) Spin polarization curves along b , a and c directions, obtained by averaging the same-color curves in (c - e), respectively. Since the background part (< -0.15 eV) should show no spin polarization, we subtracted a constant for all the curves to remove the background spin polarization.

References:

- [1] R. Noguchi, et al. Nature 566, 518 (2019).
- [2] H. Weng, Dai, X. & Fang, Z. Phys. Rev. X 4, 011002 (2014).

Observation of spin polarized surface states in polar Weyl semimetal T_d -MoTe₂

M. Sakano¹, Y. Tanaka¹, M. S. Bahramy^{1,2}, H. Takahashi^{1,3}, K. Kuroda⁴, A. Harasawa⁴, K. Yaji⁴, S. Shin⁴, S. Ishiwata^{1,3}, K. Ishizaka^{1,2}

¹*Quantum-Phase Electronics Center (QPEC) and Department of Applied Physics, The University of Tokyo*

²*RIKEN Center for Emergent Matter Science (CEMS)*

³*Graduate School of Engineering Science, Osaka University*

⁴*Institute for Solid State Physics, The University of Tokyo*

The electronic structure in the low temperature phase of T_d -MoTe₂, which is theoretically predicted as a type-II Weyl semimetal, has been intensively investigated by angle-resolved photoelectron spectroscopy [1-6]. Until now, some segment-like band features resembling Fermi arcs are experimentally observed, which are indicative of the topological surface states connecting the bulk Weyl nodes [5,6]. However, since the complicated electronic structure near the Fermi level makes it difficult to be observed, the interpretations of ARPES results on the observed Fermi-arc-like bands are still controversial. Here we investigate the spin polarizations of the Fermi arc features for both polar terminations by utilizing the high-resolution spin and angle-resolved photoelectron spectroscopy (SARPES) [7].

T_d -MoTe₂ has the noncentrosymmetric crystal structure with polarization along the stacking direction (c -axis), so it has the “top” and “bottom” polar domains. The top surface is denoted by (001) and the bottom surface is denoted by (00-1). According to the band calculations, there are eight Weyl points in the first Brillouin zone of T_d -MoTe₂. Their energy levels and coordinates are predicted to be $(E, k_x, k_y, k_z) = (E_F + 6.7 \text{ meV}, \pm 0.185, \pm 0.013, 0)$ (W1s : near the Γ -X line) and $(E_F + 59 \text{ meV}, \pm 0.181, \pm 0.053, 0)$ (W2s : the far from Γ -X line) by the theoretical research[21]. Fig. 1(a) and (b) show the energy contours at $E_F + 6.7 \text{ meV}$ for the (001) and (00-1) surfaces respectively. On the (001) surface, an arc-like surface state dispersing from the W1 can be seen between the hole pocket and the electron pocket. In addition, there is another surface state that crosses the Γ -X line near the electron pocket, indicated by “SS”. On the (00-1) surface, there is a sharp surface state that connects the pair of W1s with different chirality, indicated by the white arrow in Fig. 1(b).

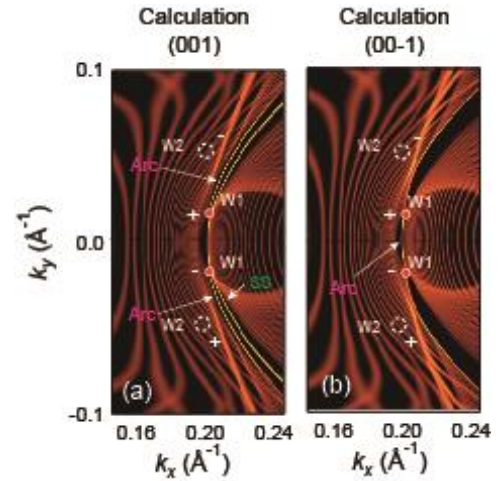


Fig. 1 The calculated energy contour at $E_F + 6.7 \text{ meV}$ for (001) (a) and (00-1) (b) surfaces.

Fig. 2(a) shows the energy contour at E_F on the (001) surface obtained by ARPES at 20 K. The two types of sharp photoelectron intensities are observed indicated by the pink solid brackets and the green curve. The pair of segments is the possible Fermi arcs connecting W1 and W2 from the comparison with the calculation shown in Fig. 1(a). The state indicated by the green curve is also a surface state but can be distinguished from the Fermi arc.

Next, looking at the energy contours at $E_F + 20 \text{ meV}$ for the (00-1) surface shown in Fig. 2(b), a short segment of the photoelectron intensity can be observed at $k_x \sim 0.20 \text{ \AA}^{-1}$ along the Γ -X line, as indicated by the pink marker. This segment is the possible Fermi arc connecting the pair of W1 across the Γ -X line, as shown in the calculation for the (00-1) surface (Fig. 1(b)).

To investigate the spin structures of the topological surface states, we perform SARPES along Fermi arcs and the SS. On the (001) surface, the SARPES measurements were performed along the orange lines (#0~#7) shown in Fig 2(a). Figs. 2(c)~(e) show the spin-resolved spectrums along #0 ~ #7 for the S_x , S_y and S_z respectively. The measurement position (#0 ~ #7) in momentum space is calculated from

the detector angle shown on the horizontal axis of Figs. 2(c)-(e). The red and blue curves represent the photoelectron intensities of the up spins and down spins, respectively. From the ARPES results shown in Fig. 2(a), there are the Fermi arc and the SS, on #0, #2~#7. The peak positions shown in the spin resolved momentum distribution curves (MDCs) are the Fermi arc and SS peak positions obtained by fitting the MDCs by the normal ARPES measurement shown in Fig 2(a). In the spin-resolved spectrums for S_x shown in Fig. 2(c), the only one peak is observed on the #1, whereas two peak structures are observed on the #2 reflecting the two different surface states, so we can say that the Arc and the SS can be measured by SARPES. The spin resolved MDCs for S_y (Fig. 2(d)) shows that the SS has S_y up polarization on the Γ -X line, the up-spin spectrums have the two-peak structure in the region slightly off the Γ -X line (#2-#5), so we can see that the S_y of the Fermi arc near W1 is up on the (001) surface. For S_z , the Arc and SS seem to have the opposite polarization near the Γ -X line, but they have large S_z -up polarization far from the Γ -X line. Next, we move on to the results of the (00-1) surface. Fig. 2(b) shows the energy contour at $E_F + 20$ meV on the (00-1) surface. SARPES is performed along the orange line in Fig. 2(b), so the peak in the 3D spin-resolved MDCs shown in Fig. 2(f)-(h) corresponds to the peak of the Arc. There seem to be no difference in the photoelectron intensities of the up and down of S_x , but the MDC of S_y -down ARPES intensities shown in Fig. 2(g) has a sharp peak which is consistent with the peak position of the Arc observed by the normal ARPES. Finally, the MDC of S_z -up ARPES intensities shown in Fig. 2(h) has a peak structure at the same position with the result of the normal ARPES, so we can see the Arc have the small S_z -down polarization.

We focus on the spin components along y of the Arc in the vicinity of the Γ -X line. The Arc of the (001) surface has S_y -up polarization ($P_y \sim 0.4$) just outside of the pair of W1 at $k_y \sim \pm 0.01 \text{ \AA}^{-1}$. On the other hand, the Arc on the (00-1) surface at $k_y = 0$ has S_y -down polarization ($P_y \sim -0.6$). In other words, the sign of the spin polarizations of the Fermi arcs on the top and bottom surface reverse at the W1s, the junction point between the Arcs. This feature seems to reflect the Berry flux emerging from the Weyl points, as the source and sink of Berry flux in momentum space.

REFERENCES

- [1] A. A. Soluyanov, *et al.*, Nature **527**, 495(2015).
- [2] Y. Sun, *et al.*, Phys. Rev. B **92** 161107 (2015).
- [3] Z. Wang, *et al.*, Phys. Rev. Lett. **117**, 056805(2015).
- [4] L. Huang, *et al.*, Nat. Mater. **15**, 1155 (2016).
- [5] A. Tamai, *et al.*, Phys. Rev. X **6**, 031032 (2016).
- [6] M. Sakano, *et al.*, Phys. Rev. B **95**, 121101 (2017).
- [7] K. Yaji *et al.*, Rev. Sci. Instrum. **87**, 053111 (2016).

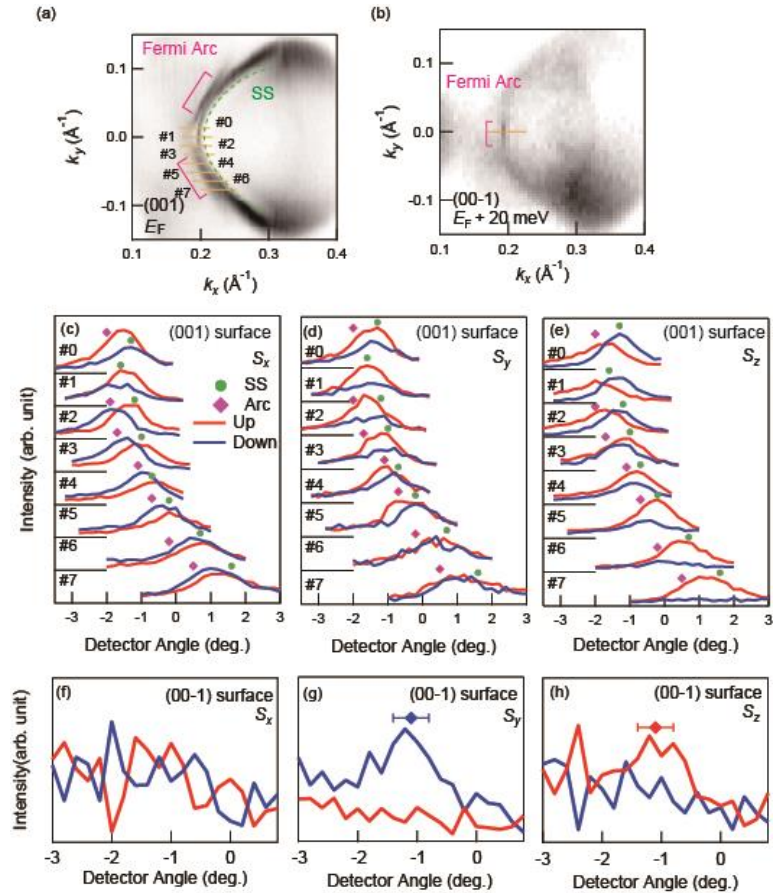


Fig.2 ARPES energy contour at E_F for (001) (a) and at $E_F + 20$ meV for (00-1) (b). (c)-(e) 3D SARPES momentum distribution curves along the orange lines in (a). (f)-(h) 3D SARPES momentum distribution curves corresponding to the orange line in (b).

SARPES STUDY OF A PB ATOMIC LAYER ON GE(111)

Koichiro Yaji¹ and Fumio Komori²

¹Research Center for Advanced Measurement and Characterization,
National Institute for Materials Science

²Division of Nanoscale Science, Institute for Solid State Physics, The University of Tokyo

Strongly spin-orbit coupled materials, such as topological insulators and Rashba systems, are placed at a central research field in condensed matter physics not only because of fundamental interests but also spintronic applications. In the standard model of the strongly spin-orbit coupled systems, the spin direction is perpendicular to both the direction of surface normal and the momentum of an electron. Recently, in contrast to the scenario of the spin-momentum locking, the spin-orbital locking model was reported in several papers [1]. Also, in our previous studies [2,3], we demonstrated the spin-orbit coupling of surface states on Bi(111) and Bi₂Se₃ with spin- and angle-resolved photoemission spectroscopy using a vacuum ultraviolet laser (laser-SARPES). Here we show the spin-orbit coupling of surface states of a monolayer Pb film on Ge(111) (Pb/Ge(111)- β) investigated by laser-SARPES. Moreover, we demonstrate the incident-light-angle dependence of SARPES.

SARPES measurements were performed at E-building in the Institute for Solid State Physics [4]. The Pb/Ge(111) sample was *in-situ* prepared in a molecular beam epitaxy chamber which was directly connected to the analysis chamber. We used an *n*-type Ge(111) substrate. The clean surface was obtained with the several cycles of Ar⁺ ion sputtering with the ion energy of 0.5 kV and subsequent annealing at 600 °C. Pb was evaporated from an aluminum crucible. The thickness of Pb and the orderliness of the monolayer film was judged from low-energy-electron-diffraction pattern. The photoelectrons were excited by 6.994-eV photons and were analyzed with a ScientaOmicron DA30-L analyzer equipped with very-low-energy-electron-diffraction type spin detectors. The electron deflector function is useful for studying the light-incident-angle dependence of SARPES. The effective Sherman function was 0.28. The sample temperature was kept at 40K during the measurements.

Figure 1 shows an ARPES image recorded along Γ K in the surface Brillion zone of Pb/Ge(111)- β , being parallel to the mirror plane of the surface. We find several bands around Γ , which are ascribed to the subsurface states of Ge(111) [5]. The bands crossing the Fermi level (E_F) around $k \sim 0.40$ - 0.45 \AA^{-1} are Pb-derived states, where the splitting is due to the Rashba effect [6]. The bands lying in the energy range of 0.3-0.8 eV below E_F around $k > 0.3 \text{ \AA}^{-1}$ are also Pb-derived states and show semiconducting behavior. The overall shapes of the bands observed with $h\nu = 6.994 \text{ eV}$ well agree with those with $h\nu = 21 \text{ eV}$ reported in our previous study [7].

The SARPES measurements were performed with p- and s-polarized lights [Fig. 2], which could be regarded as orbital-selective SARPES. Here, the light incident angles were set to 20° and 40°. We used the spin detector for resolving the *y*-spin component, which was perpendicular

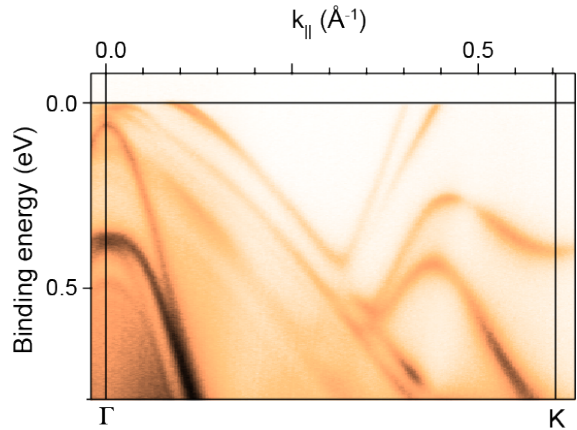


Fig. 1 The ARPES image of Pb/Ge(111)- β along Γ K recorded with the photon energy of 6.994 eV. The color arrangement gives the information of the photoelectron intensity.

to the mirror plane of the surface. As shown in Fig. 2, we clearly demonstrate that the observed spin polarizations are inverted upon switching the light polarizations. This indicates that the symmetric and anti-symmetric orbitals are independently coupled to mutually opposite spins as in other spin-orbit coupled systems such as Bi(111) and Bi₂Se₃. The total spin polarization is obtained from the integrations of the orbital-selective spin polarizations with p- and s-polarized lights. For the light incident angle of 20°, the spin-polarized branches show opposite spin directions each other, which is in agreement with the scenario of the Rashba effect. On the other hand, for the 40° incidence, the total spin polarizations are in the same directions, which is against the Rashba scenario and violates the time reversal symmetry. Besides, the theoretical calculation suggests that these branches exhibit the Rashba-type spin texture [7]. Therefore, we conclude that the spin polarization observed with SARPES with the incident angle of 40° is largely influenced by the final-state effect in photoemission process. It is likely that the photoionization cross sections between the p- and s-polarizations are different. We have to mind that the total spin polarization is not always derived from the integrations of the orbital-resolved ones.

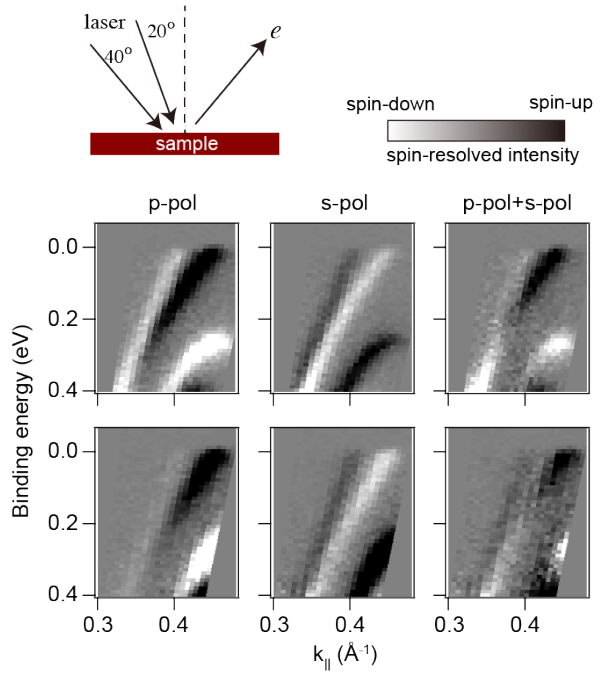


Fig. 2 Laser-SARPES images for the Pb-derived surface states along ΓK recorded with the light incident angles of 20° (upper panels) and 40° (lower panels) with the p-polarized light (left panels) and the s-polarized light (center panels). The right panels represent the orbital-integrated SARPES image. White and black colors give the information of the negative-positive spin polarizations. The left-upper panel is a schematic drawing of the experimental geometry.

REFERENCES

- [1] Z.-H. Zhu et al., Phys. Rev. Lett. **110**, 216401 (2013), Y. Cao et al., Nat. Phys. **9**, 499 (2013), H. Zhang et al., Phys. Rev. Lett. **111**, 066801 (2013), Z. Xie et al., Nat. Commun. **5**, 3382 (2014).
- [2] K. Kuroda et al., Phys. Rev. B **94**, 165162 (2016).
- [3] K. Yaji et al., Nat. Commun. **8**, 14588 (2017).
- [4] K. Yaji et al., Rev. Sci. Instrum. **87**, 053111 (2016).
- [5] K. Yaji et al., J. Electron Spect. Rel. Phenom. **201**, 92 (2015).
- [6] K. Yaji et al., Nat. Commun. **1**, 17 (2010).
- [7] K. Yaji et al., Phys. Rev. B **86**, 235317 (2012).

HIGH-RESOLUTION SPIN-RESOLVED ELECTRONIC STRUCTURE OF TOPOLOGICAL HEAVY-FERMION MATERIALS

Andrés F. Santander-Syro, Franck Fortuna, Maximilian Thees

Institut des Sciences Moléculaires d'Orsay (ISMO), Université Paris-Saclay and CNRS, France

Cris Adriano

Instituto de Física “Gleb Wataghin”, UNICAMP, Campinas-SP, 13083-859, Brazil

Ce-based intermetallic compounds have interesting physical properties that arise from the interplay between Ruderman-Kittel-Kasuya-Yoshida (RKKY) magnetic interaction, crystalline electric field and Fermi surface (FS) effects in connection to a strong hybridization between the Ce^{3+} $4f$ electrons and the conduction electrons. Ce-based materials often present non-trivial ground states, such as heavy fermion, unconventional superconductivity and non-Fermi-liquid behavior, which frequently appear in the vicinity of a magnetically ordered state. Interestingly, some of these properties, seem to be favored to occur in low symmetry systems such as tetragonal structure, well-known examples are the families of CeMIn_5 , Ce_2MIn_8 ($M = \text{Co}, \text{Rh}, \text{Ir}, \text{Pd}$), CePt_2In_7 and CeCuSi_2 .

In this context, recent attention was given to the CeTX_2 family ($T =$ transition metal; $X =$ pnictogen), which hosts both ferromagnetic (FM) and antiferromagnetic (AFM) members with complex magnetic behavior [1]. In particular, in this project we investigated, using laser-excited spin- and angle-resolved photoemission spectroscopy (Laser-SARPES), the compound CeCuBi_2 that crystallizes in the tetragonal ZrCuSi_2 -type structure (P4/nmm [1]). Previous studies show that CeCuBi_2 has an AFM ordering at $T_N = 16$ K with a large magnetic anisotropy [1].

As shown in Figure 1, in the AFM phase we detected a dispersive hole-like state with a finite spin polarization. This state may arise from unpaired or incompletely paired moments near the material surface, as also observed in other AFM heavy-fermion systems [2]. Further data analyses and complementary spin-integrated ARPES measurements are currently being performed to clarify its origin.

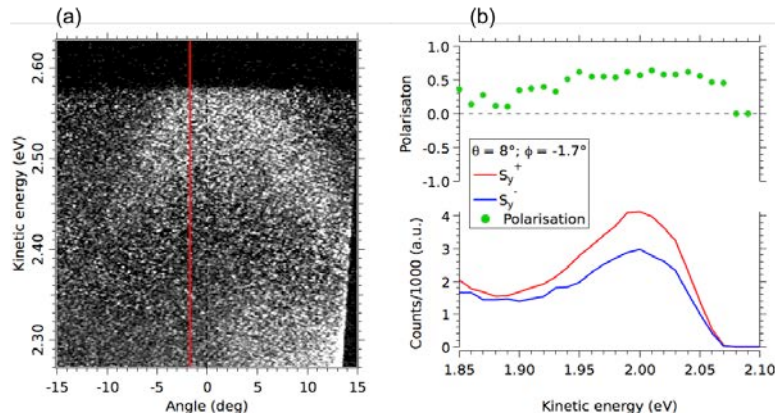


Figure 1. (a) laser-ARPES energy-momentum map showing a hole-like state right below the Fermi level in CeCuBi_2 . (b) Bottom panel: spin-resolved energy distribution curves along the momentum marked by the red line in (a); top panel: net spin polarization.

REFERENCES

[1] Cris Adriano et al., Phys. Rev. B **90**, 235120 (2014).

[2] A. Chikina et al., Nat. Commun. **5**, 1-7 (2014).

Study of spin structure in domain-regulated alloy of atomic layer

Ting-Yu Chen¹, Li-Cheun Yang², Santosh Chiniwar¹, H. -T. Jeng¹, Woei Wu Pai³, S. -J. Tang^{1,2},

1. *Department of Physics, National Tsing Hua University, Hsinchu 30013, Taiwan*

2. *National Synchrotron Radiation Research Center (NSRRC), Hsinchu 30076, Taiwan*

3. *Center for Condensed Matter Sciences, National Taiwan University, Taipei 106, Taiwan*

The enhanced Rashba effect of a 2-dimensional (2D) surface alloy has been a center of interest in surface-science community. A typical Rashba effect in a 2D system is mainly contributed by the out-of-plane electric field caused by the inversion–symmetry breaking perpendicular to the surface plane. Consequently, the k momentum of degenerate surface-state bands locked with opposite in-plane spin polarizations shift in positive and negative directions, respectively, forming a concentric 2D constant-energy contour (CEC). However, previous studies on 2D surface alloys revealed the enhanced Rashba effect correlated with possible in-plane electric field and thus out-of-plane spin polarizations. Such effect was attributed to the second-order warping term of spin-orbit interaction in addition to the first-order term for the typical Rashba effect.

Our group found that the surface-state bands of GeAg₂ surface alloy formed on Ag(111) exhibits anomalous splitting centered at surface zone center $\bar{\Gamma}$ as shown in Fig. 1. The splitting is obvious in one symmetry direction $\bar{\Gamma}\bar{M}_{Ag_2Ge}$ but negligible in another $\bar{\Gamma}\bar{K}_{Ag_2Ge}$. The corresponding 2D CECs centered at $\bar{\Gamma}$ is displayed in Fig. 2(a), exhibiting an entangled configuration of inner hexagon and outward snowflakes that rotate 30° with each other.

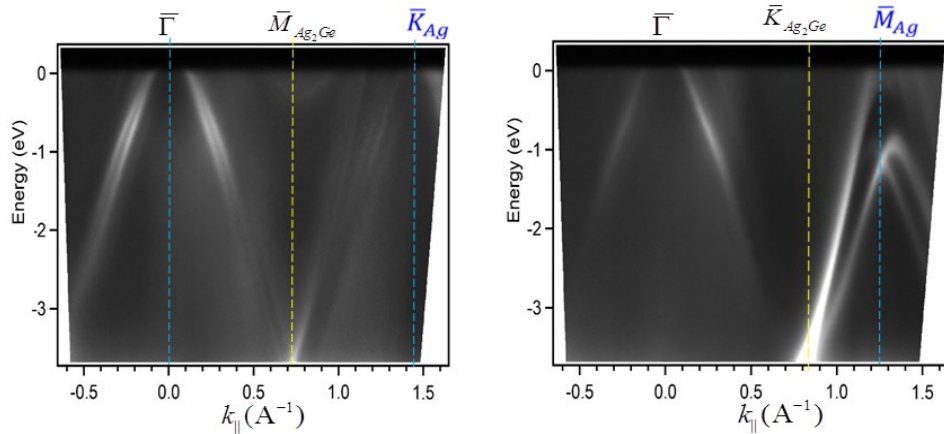


Fig. 1: The measured energy band dispersions for Ag₂Ge on Ag(111) in two symmetry directions

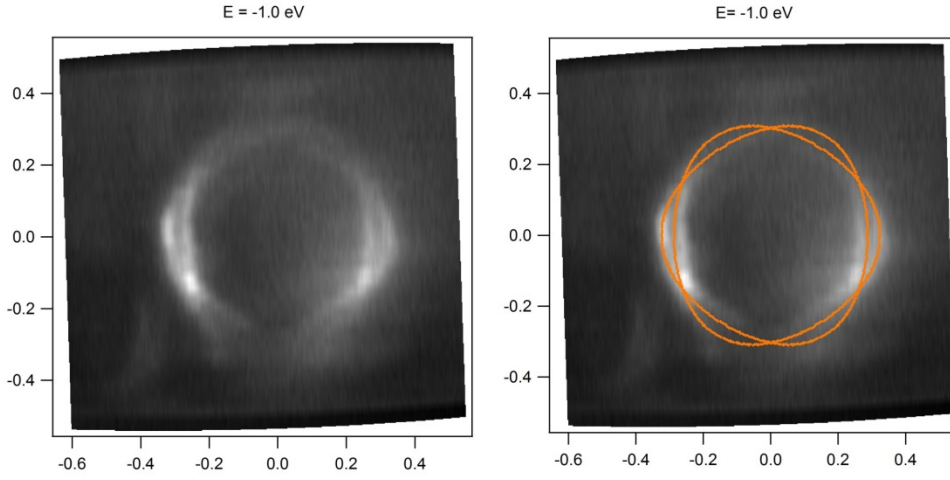


Fig. 2: (a) The measured 2D constant energy contours at -1.0 eV for surface-state bands of Ag_2Ge surface alloy on $\text{Ag}(111)$ centered at $\bar{\Gamma}$ and (b) the corresponding fitting result.

We employed the spin-orbit interacting model of the first-order Rashba term and the second-order Warping term to simulate the measured CECs in Fig. 2(a); the match is very agreeable as shown by the orange fitting curve in Fig. 2(b). Moreover, the fitting result shows that the contribution to the splitting is dominantly from the Warping term, being in complete contrast to the behaviors in most surface alloys where the first-order Rashba term dominates. If it is the case, the spin polarizations of the surface-state bands of Ag_2Ge surface alloy centered at $\bar{\Gamma}$ would be dominantly out-of-plane. This motivated us to come to the Synchrotron Radiation Laboratory in the Institute for Solid State Physics, The University of Tokyo, Japan to use the spin- and angle-resolved photoelectron spectroscopy (SARPES) to measure the spin texture of surface state bands of Ag_2Ge surface alloy. Figure 3 shows the scanning-tunneling-microscopy (STM) image of Ag_2Ge surface alloy coexisting with striped-phase germanene which form triangle arrays enclosing the Ag_2Ge surface alloy. We believe the triangle arrays break the in-plane symmetry to cause the in-plane electric field.

Figure 4 shows the preliminary results of our spin-resolved photoemission measurement carried out in SARPES machine time in Nov 2019. The applied magnetic field was along the out-of-plane direction (z direction). Indeed one can see the energy distribution curves (EDCs), taken at off-normal 8° , corresponding to two opposite directions ($\pm z$) of magnetic fields reveal difference in intensities for the two peaks of the split surface-state bands. However, it is a bit abnormal that the two peaks of red EDC are both higher than those of blue EDC. I think the surface normal of our sample was not completely aligned with the detector axis during measurement. In our next SARPES machine, we will be much more careful in those measurement details.

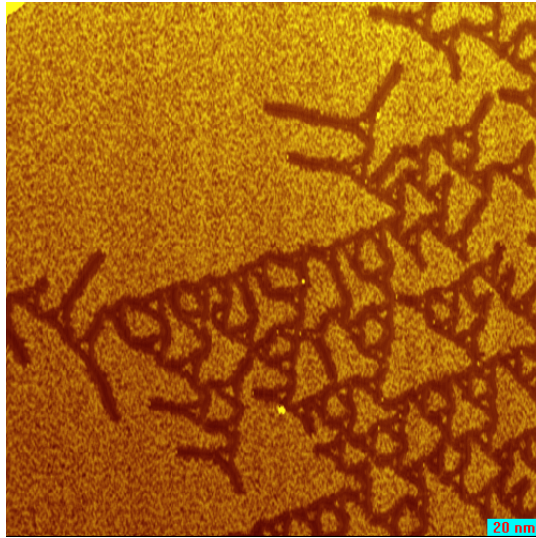


Fig. 3: The STM image of Ag₂Ge surface alloy coexisting with striped-phase germanene in the form of triangle arrays.

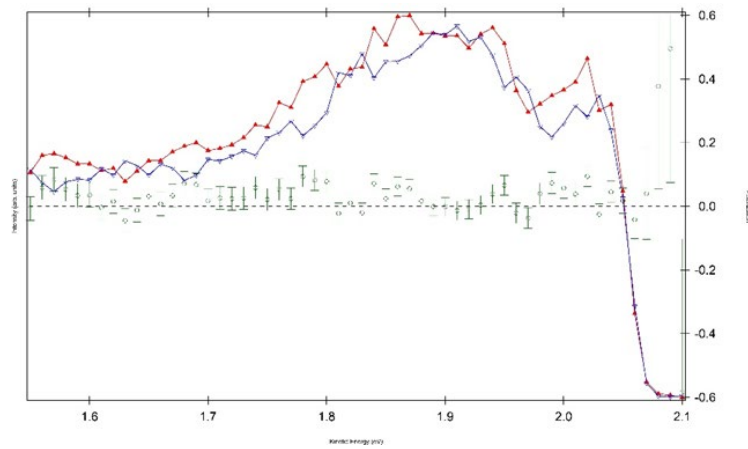


Fig. 4: The preliminary result of spin-resolved photoemission measurement on the split surface-state bands of Ag₂Ge surface alloy. Red and blue EDCs correspond to opposite directions ($\pm z$) of magnetic fields.

Spin resolved ARPES on interfacial electronic states of Bi/NbSe₂

R. Stania¹, H. Jung^{1,2}, H.W. Yeom^{1,2}

¹*Center for Artificial Low Dimensional Electronic Systems, Institute for Basic Science (IBS), Pohang 37673, Republic of Korea*

²*Department of Physics, Pohang University of Science and Technology (POSTECH), Pohang 37673, Republic of Korea*

Introduction

Bulk, as well as low-dimensional, bismuth (Bi) have provided extremely rich platforms to advance our knowledge in condensed matter physics, ranging from high thermoelectric properties[1] to giant Rashba effect with highly spin-polarized electrons [2][3]. Moreover, there have recently been much interest in the topological classification of Bi, and it has been reported that pure Bi is topologically non-trivial in bulk [4][5], as well as in thin film[6]. More recently, it has also been reported that due to the higher-order topology, Bi also possesses topologically protected hinge (edge) states even in bulk form [7]. Such new identifications of Bi are expected to open up further possibilities for Bi-based structures, particularly when combined with other novel materials.

In order to utilize the rich properties of Bi-based structures, both to explore further fundamental aspects and for future device applications, it is essential to understand the electronic interactions of low-dimensional Bi on various substrates, particularly at their interfaces (e.g., topological quantum computations when combined with superconductors [7]). Of special interest are two-dimensional (2D) layered van-der-Waals materials (vdW) which are known to host exceptional spin-related properties and have strong potential for spintronic applications [8].

Thus, in our experiments, we aimed to investigate the electronic structures of ultra-thin Bi and its interfacial electronic states on a transition metal dichalcogenide (TMDC). In particular, 2H-NbSe₂ not only shows a phase transition from metallic state to charge density wave (CDW) state [9], but also towards superconducting state at one of the highest transition temperatures amongst the TMDCs [10]. In addition, NbSe₂ was recently predicted to be topologically non-trivial [11]. Thus, Bi/NbSe₂ is an ideal playground to explore such interactions and an important step towards the investigation of topological superconductivity and Majorana fermions.

Experimental details

The NbSe₂ samples were cleaved under UHV conditions and the surface quality was confirmed using LEED and He II α . The Bi layers were grown in a separate chamber and coverage was determined using He II α excitation. The high resolution ARPES and SARPES measurements were performed using a laser light source with a photon energy of 6.994 eV at the laser-SARPES machine developed at ISSP [12]. All photoemission experiments were carried out at sample temperatures below 35 K under UHV condition (about 1×10^{-8} Pa).

Results and discussion

By using high resolution ARPES we were able to distinguish the bands around the Γ point which not only shows the expected bands for freestanding few-layer Bi(111) but also additional bands that could not be clearly allocated and may resemble interface states (Figure 1a). Spin dependent measurements reveal a strong spin texture (Figure 1b) for the TSS around $E_B=0.7$ eV and especially for the surface state near the Fermi level, which was expected to be less strong polarized for few BL Bi films. More structural investigation and theoretical calculation will be required in order to determine the origins of the sub-bands.

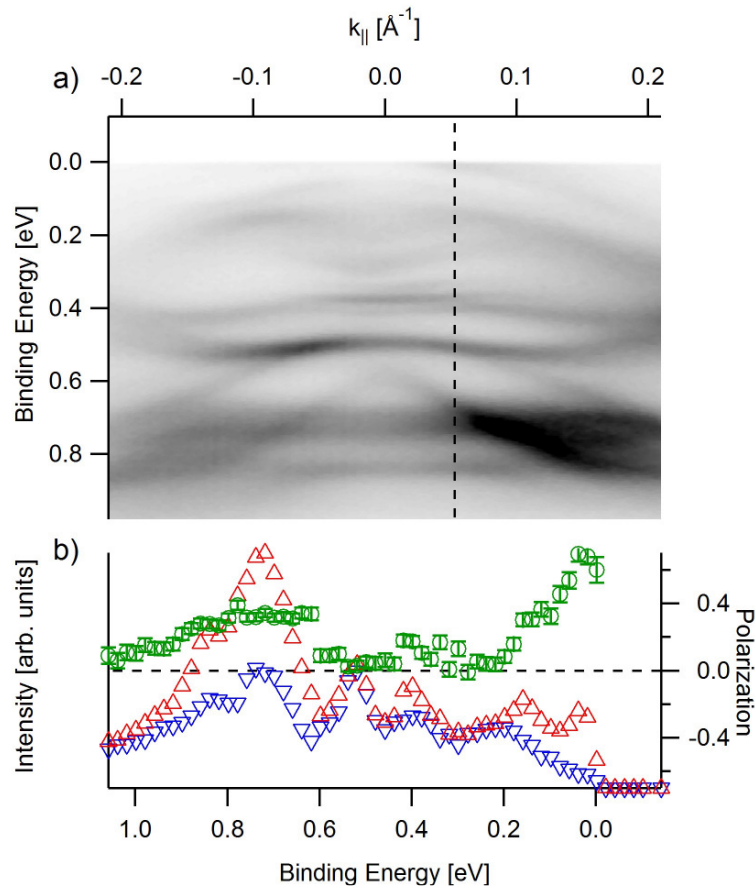


Fig. 1 a) Spin integrated measurement of Bi/NbSe₂ along the ΓK direction; b) spin dependent EDC along the dashed line in a) with red (blue) corresponding to out of plane spin up (down) measurements and green the polarization

References

- [1] B. Poudel, *et al.*, Science, **320**, 634 (2008)
- [2] Y. Koroteev, *et al.*, Phys. Rev. Lett., **93**, 046403 (2004)
- [3] T. Hirahara, *et al.*, Phys. Rev. B, **76**, 153305 (2007)
- [4] S. Ito, *et al.*, Phys. Rev. Lett., **117**, 35 (2016)
- [5] Y. Ohtsubo, *et al.*, New J. Phys., **18**, 123015 (2016)
- [6] I.K. Drozdov, *et al.*, Nat. Phys., **10**, 664 (2014)
- [7] F. Schindler, *et al.*, Nat. Phys., **14**, 918 (2018)
- [8] D. Pensin, A.H. MacDonald Nature Mater., **11**, 409 (2012)
- [9] D.E. Moncton, *et al.*, Phys. Rev. Lett., **34**, 734 (1975)
- [10] R. F. Frindt Phys. Rev. Lett., **28**, 299 (1972)
- [11] M. S. Bahramy, *et al.*, Nature Mater., **17**, 21 (2017)
- [12] K. Yaji, *et al.*, Rev. Sci. Instrum., **87**, 053111 (2016)

HIGH-RESOLUTION SPIN- AND ANGLE-RESOLVED PHOTOEMISSION SPECTROSCOPY ON DOPED MAGNETIC TOPOLOGICAL INSULATORS

Keisuke Fukutani^{1,2}, Chandan De¹, Roland Stania^{1,2}, Koichiro Yaji³, Kenta Kuroda³,
Jaeyoung Kim^{1,2}, and Han-Woong Yeom^{1,4}

¹*Center for Artificial Low dimensional Electronic Systems, Institute for Basic Science (IBS), Republic of Korea*

²*Pohang Accelerator Laboratory, Pohang University of Science and Technology (POSTECH), Republic of Korea*

³*The Institute for Solid State Physics, The University of Tokyo, Japan*

⁴*Department of Physics, Pohang University of Science and Technology (POSTECH), Republic of Korea*

The topological classifications in condensed matter physics have led to a paradigm shift in our understanding of the properties of solids, where the fundamental characteristics of matters can be determined not only by their symmetries and many-body interactions but also by their topological orders [1]. Such new classification schemes, have allowed for the predictions and discoveries of various new types of materials, leading to the realizations of intriguing electronic properties [2-7]. Among them, the interplay between the topological order and magnetism (broken time-reversal symmetry) has garnered much attentions as it is expected to lead to various exotic phenomena, such as quantum anomalous Hall effect [8] and topological magnetoelectric effect [9], and have been extensively studied to date [10].

Recently, a discovery of an intrinsic antiferromagnetic topological insulator MnBi_2Te_4 has been reported [11-13], followed by extensive investigations by various experimental and theoretical means on this material as well as its hetero-structural cousins $(\text{MnBi}_2\text{Te}_4)_n(\text{Bi}_2\text{Te}_3)_m$ [14-17]. On the other hand, despite the expected broken time-reversal symmetry, the electronic band structures of these materials are variously reported with regard to the presence of the band gap in the Dirac cone [18-23], which is at the heart of topological electronic properties. While there are several proposed hypotheses to explain such discrepancies [20,22,23], the general consensus has not been reached.

The keys to resolve such issue can be provided by high-resolution spin- and angle-resolved photoemission spectroscopy (SARPES), which allows us to simultaneously probe the topological surface Dirac band and their momentum-dependent spin textures. Since it is known for these materials that the microscopic domain sizes and the presence of bulk band projections, pronounced above the photon energies of $h\nu \sim 10$ eV [11], can obscure the unambiguous observation of the Dirac bands, utilizations of the micro-spot-sized, laser-based ($h\nu = 7$ eV) SARPES available at the Institute for Solid State Physics (ISSP) at the University of Tokyo would be an ideal experimental probe to tackle the present issue.

In our experiments, we have performed laser-SARPES measurements on the pristine as well as Sb-doped $(\text{MnBi}_2\text{Te}_4)_n(\text{Bi}_2\text{Te}_3)_m$ at the temperatures above and below the magnetic phase transition temperatures and have revealed their electronic structures as well as the corresponding spin textures near the Γ point in the surface Brillouin zone. Fig. 1 shows the ARPES intensity plots and the corresponding Fermi surface mapping for the pristine MnBi_2Te_4 and MnBi_4Te_7 . It can be clearly seen that the both materials possess *gapless* Dirac cones centered at the Γ point with the Dirac point (E_D) located at the binding energy of ~ 2.7 eV with no clearly identifiable band gap. These observations are consistent with some of the earlier ARPES studies [20-23], and likely point to the possibility that near the surface, the magnetic configurations are different from that of the bulk (i.e., possible surface magnetic

reconstructions), so as to provide the effective protection from gap-opening even in the absence of the time-reversal symmetry [15]. In order to identify the magnetic configurations near the surface and to identify the possible origin of the gapless Dirac cones, we have further obtained the spin-resolved ARPES data for the pristine as well as the Sb-doped samples. The spin-resolved data show unconventional spin textures for topological surface states and are currently under further investigation in conjunction with theoretical calculations as well as transport measurements.

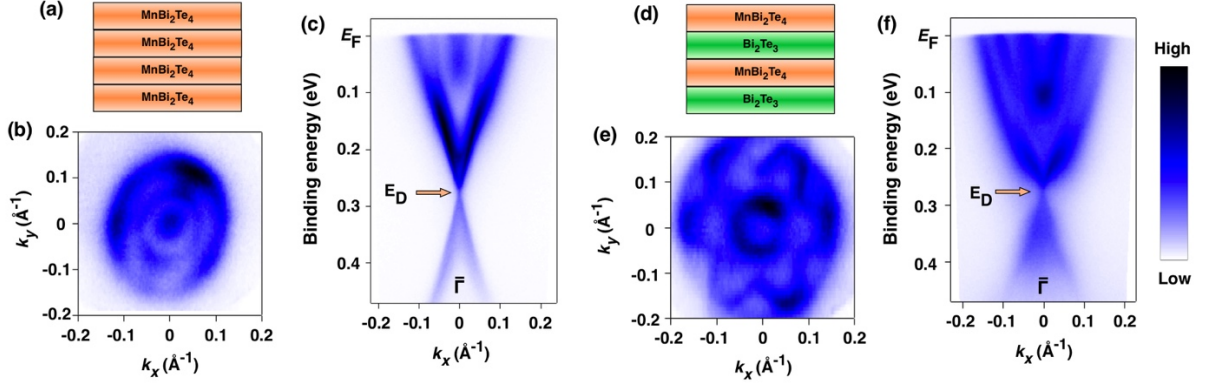


Figure 1: ARPES intensity maps for (a-c) MnBi_2Te_4 and (d-f) MnBi_4Te_7 . (a) and (b) schematically show the layer-stacking sequences for each of the materials, where the topmost layers are determined to be both MnBi_2Te_4 . (b) and (e) show the Fermi surface mappings and (c) and (f) show the band dispersions around the Γ point. The Dirac point E_D , where the upper and lower Dirac cones meet in the gapless dispersions are indicated by the arrows for both materials. The data were obtained with the s -polarized 7-eV laser at the temperature of $T = 10$ K.

REFERENCES

- [1] M. Z. Hasan and C. L. Kane, *Rev. Mod. Phys.* **82**, 3045 (2010).
- [2] C.-Z. Chang *et al.*, *Science* **340**, 167 (2013).
- [3] C.-K. Chiu *et al.*, *Rev. Mod. Phys.* **88**, 035005 (2016).
- [4] P. Zhang *et al.*, *Science* **360**, 182 (2018).
- [5] C.X. Trang *et al.*, *Nat. Commun.* **11**, 159 (2020).
- [6] L. Fu *et al.*, *Phys. Rev. Lett.* **100**, 096407 (2008).
- [7] A. Das *et al.*, *Nat. Phys.* **8**, 887 (2012).
- [8] F. D. M. Haldane, *Phys. Rev. Lett.* **61**, 2015 (1988).
- [9] X.-L. Qi *et al.*, *Phys. Rev. B* **78**, 195424 (2008).
- [10] Y. Tokura *et al.*, *Nat. Rev. Phys.* **1**, 126 (2019).
- [11] M. M. Otrokov *et al.*, *Nature* **576**, 416 (2019).
- [12] E. D. L. Rienks *et al.*, *Nature* **576**, 423 (2019).
- [13] Y. Gong *et al.*, *Chinese Phys. Lett.* **36**, 076801 (2019).
- [14] R. C. Vidal *et al.*, *Phys. Rev. X* **9**, 041065 (2019).
- [15] Y.-J. Hao *et al.*, *Phys. Rev. X* **9**, 041038 (2019).
- [16] L. Ding, *et al.*, *Phys. Rev. B* **101**, 020412(R) (2020).
- [17] R. C. Vidal *et al.*, *Phys. Rev. B* **100**, 121104 (2019).
- [18] J. Wu *et al.*, *Science Advances* **5**, eaax9989 (2019).
- [19] K. N. Gordon *et al.*, arXiv:1910.13943 (2019).
- [20] P. Swatek *et al.*, *Phys. Rev. B* **101**, 161109(R) (2020).
- [21] B. Chen *et al.*, *Nat. Commun.* **10**, 4469 (2019).
- [22] Y.J. Chen *et al.*, *Phys. Rev. X* **9**, 041040 (2019).
- [23] Y. Fu *et al.*, *Phys. Rev. B* **101**, 161113(R) (2020).